EFDA–JET–CP(12)06/36

M. Groth, S. Brezinsek, P. Belo, M.N.A. Beurskens, M. Brix, M. Clever, J.W. Coenen, C. Corrigan, T. Eich, J. Flanagan, C. Guillemaut, C. Giroud, D. Harting, A. Huber, S. Jachmich, K.D. Lawson, M. Lehnen, C. Lowry, C.F. Maggi, S. Marsen, A.G. Meigs, R.A. Pitts, G. Sergienko, B. Sieglin, C. Silva, A. Sirinelli, M.F. Stamp, G.J. van Rooij, S. Wiesen and JET EFDA contributors

Impact of Carbon and Tungsten as Divertor Materials on the Scrape-Off Layer Conditions in JET

Impact of Carbon and Tungsten as Divertor Materials on the Scrape-Off Layer Conditions in JET

M. Groth[1], S. Brezinsek[2], P. Belo[3], M.N.A. Beurskens[4], M. Brix[4], M. Clever[2], J.W. Coenen[2], C. Corrigan[4], T. Eich[5], J. Flanagan[4], C. Guillemaut[6], C. Giroud[4], D. Harting[2], A. Huber[2], S. Jachmich[7], K.D. Lawson[4], M. Lehnen[2], C. Lowry[8], C.F. Maggi[5], S. Marsen[9], A.G. Meigs[4], R.A. Pitts[10], G. Sergienko[2], B. Sieglin[5], C. Silva[3], A. Sirinelli[4], M.F. Stamp[4], G.J. van Rooij[11], S. Wiesen[2] and JET EFDA contributors*

JET-EFDA, Culham Science Centre, OX14 3DB, Abingdon, UK

[1]Aalto University, Association EURATOM-Tekes, Espoo, Finland
[2]Institute for Energy and Climate Research, Association EURATOM-FZJ Jülich, Germany
[3]Institute of Plasmas and Nuclear Fusion, Association EURATOM-IST, Lisbon, Portugal
[4]EURATOM-CCFE Fusion Association, Culham Science Centre, OX14 3DB, Abingdon, OXON, UK
[5]Max-Planck Institute for Plasma Physics, EURATOM-Association, Garching, Germany
[6]Association Euratom CEA, CEA/DSM/IRFM, Cadarache, France
[7]Association "EURATOM Belgium State", Laboratory for Plasma Physics, Brussels, Belgium
[8]EFDA Close Support Unit, Culham Science Centre, OX14 3DB, Abingdon, OXON, UK
[9]Max-Planck-Institute for Plasma Physics, EURATOM Association, Greifswald, Germany
[10]ITER Organisation, 13115 Saint-Paul-Lez-Durance, France
[11]FOM Institute DIFFER, Association EURATOM-FOM, Nieuwegein, The Netherlands
** See annex of F. Romanelli et al, "Overview of JET Results", (24th IAEA Fusion Energy Conference, San Diego, USA (2012)).*

Preprint of Paper to be submitted for publication in Proceedings of the
24th IAEA Fusion Energy Conference (FEC2012), San Diego, USA
8th October 2012 - 13th October 2012

ABSTRACT.
The impact of carbon and beryllium/tungsten as plasma-facing components on plasma radiation, divertor power and particle fluxes, and plasma and neutral conditions in the divertors has been assessed in JET both experimentally and by simulations for plasmas in low confinement mode. In high-recycling conditions the studies show a 30% reduction in total radiation in the scrape-off layer when replacing carbon with beryllium in the main chamber and tungsten in the divertor. Correspondingly, at the low field side divertor plate a two-fold increase in power conducted to the plate and a two-fold increase in electron temperature at the strike point were measured. In low-recycling conditions the SOL was found to be nearly identical for both materials configurations. These observations are in qualitative agreement with predictions from the fluid edge code package EDGE2D/EIRENE. The rollover of the ion currents to both plates was measured to occur at 30% higher upstream densities and radiated power fraction in the Be/W configuration. Past rollover, it was possible to reduce the ion currents to the low field side targets by a factor of 2 and to operate in stable, detached conditions in the JET-ILW configuration; in the JET-C configuration the reduction was limited to 50%. Plasmas with low and high triangularity (and thus magnetic separation to the top of the device), and horizontal and vertical target configurations were investigated and compared to EDGE2D/EIRENE predictions.

1. INTRODUCTION

Radiation from impurities in the scrape-off layer (SOL) of tokamaks critically affects the SOL power balance and thus the power conducted to the divertor target plates. Carbon, in particular, strongly radiates in the temperature range characteristic of the divertor SOL (i.e., 10 to 50eV), favourable for the reduction of power conducted to the divertor target plates. When changing the plasma facing components (PFCs) from all-carbon to metals in JET (JET-C and JET-ILW, respectively) in 2009/10 in one single shutdown [1], a significant loss of carbon radiation was anticipated, which in turn, was predicted to result in higher divertor heat loads. The present JET ITER-like wall consists of beryllium in the main chamber, including bulk Be in high heat flux areas, such as limiters, and Be-coated carbon-fibre composite (CFC) surfaces in the other, recessed areas. The divertor PFCs are made of bulk W for the horizontally inclined tiles at the low field side (LFS) and W-coated CFC surfaces in all the other divertor areas, including the vertically inclined targets at both the high field side (HFS) and LFS. Sets of reference plasmas in low-confinement mode (L-mode) with moderate auxiliary power of up to 3MW were performed in both the JET-C and JET-ILW materials configurations to systematically characterise the materials effect on the SOL conditions [2]. These plasmas included attached and detached plasmas in low and high triangularity magnetic configurations ($\delta \sim 0.2$ and 0.4, respectively) and the LFS strike point connected to the horizontal plate; the HFS strike point was always connected to the HFS vertical plate (Fig.1). For simplicity, these configurations are therein named horizontal. To assess the divertor performance in ITER-relevant configurations, magnetic equilibria with both strike points on the vertical plates were also investigated. This report describes

the analysis for the radiative losses in the SOL, the particle and heat fluxes to the divertor targets, and the plasmas conditions (electron temperature, T_e) at the divertor plates, and predictions of these parameters using the fluid edge code package EDGE2D/EIRENE [3]-[5].

2. COMPARISON OF ATTACHED L-MODE PLASMAS IN THE JET-C AND JET-ILW CONFIGURATIONS

The SOL in attached (i.e., low and high recycling) divertor conditions was extensively characterised in both material configurations in low-power, neutral beam-heated L-mode plasmas; in the JET-ILW, the studies were extended toward detached plasmas. To facilitate EDGE2D/EIRENE simulations of these plasmas, a low triangularity configuration ($\delta \sim 0.2$) with a large (magnetic) clearance to the top of the vessel was chosen (Fig.1). These experiments were conducted at machine parameters typical for JET in normal current and field direction ($\mathbf{B}\times\nabla B$ toward the divertor): plasma current, I_P, of 2.5MA, toroidal field, B_T, on the magnetic axis of 2.5T, resulting in an edge safety factor, q_{95}, of 3.4. Of the total input power, ranging from 2.8 to 3.0MW and including neutral beam heating of 1.6MW, approximately 2.6 MW was transported in the SOL (Fig.2a) for all achieved upstream densities, n_{up}. Here, n_{up} refers to the line-averaged density at the edge of the core plasma (minimum normalised radius at 0.9). Different values for n_{up} were achieved by deuterium gas fuelling from the top and divertor regions: both fuelling ramps with stationary strike points, and constant fuelling for several seconds with strike point sweeps over protruding Langmuir probes embedded in the divertor targets were applied to obtain spatially resolved ion flux and T_e profiles.

In both materials configuration, the total power radiated in the SOL, $P_{rad,SOL}$, increased linearly with n_{up}, and saturated for JET-ILW as the divertor legs started to detach (Fig.2a). Integration of the radiation over the divertor legs ($P_{rad,div}$) indicated that $P_{rad,div}$ saturated before the rollover of the ion currents in JET-C (Fig.2b), and was about 30% higher than in the JET-ILW for high-recycling conditions. This observation is consistent with the reduction in the carbon content in JET-ILW measured by charge exchange and visible spectroscopy: a ten-fold decrease in the C^{6+} density at the LFS midplane and low charge state carbon emission in the LFS divertor were observed [6]. Similarly, by going from JET-C to JET-ILW the effective charge state, Z_{eff}, was reduced from 1.6 to 1.4 at the lowest n_{up}, and from 1.4 to 1.1 at medium n_{up}.

For low-recycling conditions the power conducted to the LFS plate ($P_{div,LFS}$) was nearly identical in the JET-C and JET-ILW configurations, whereas for high-recycling conditions, $P_{div,LFS}$ was about a factor of 2 lower in JET-C (Fig.2c). This observation further corroborates that more power was radiated in the SOL in JET-C compared to JET-ILW.

Nearly identical (within 50%) ion currents to the HFS and LFS plates ($I_{div,HFS}$ and $I_{div,LFS}$, respectively) were measured in attached conditions in both JET-C and JET-ILW (Fig.2d and 2e). In JET-ILW, both $I_{div,HFS}$ and $I_{div,LFS}$ continued to increase and saturated halfway through the scanned density range. It is important to note that the rollover of $I_{div,HFS}$ and $I_{div,LFS}$ occurred at the same n_{up}, at radiated power fraction of approximately 50%. In JET-ILW, the density limit was reached

at 65% of the Greenwald density and a radiated power fraction of 65%. In addition, data from the fuelling ramp showed a sharp reduction of I_{div} at slightly lower n_{up} than those observed in steady-state plasmas. Similarly, the neutral behaviour as indicated by low charge state Balmer line emission from deuterium atoms (D_α) and the neutral pressures measured in the divertor pumping plenum (data not shown) show negligible dependence on the divertor materials: for JET-ILW, both parameters increased linearly with n_{up} beyond rollover of I_{div}, and only saturate at the highest n_{up} obtained.

While in low-recycling conditions identical peak electron temperatures were measured at the LFS plate ($T_{e,LFS}$) for the two materials configurations, $T_{e,LFS}$ was found factors of 2 to 3 higher in the ILW in high-recycling conditions (Fig.2f). This observation is consistent with $P_{div,LFS}$ shown above. In JET-ILW the sharp reduction of $T_{e,LFS}$ from 25 eV to 8eV occurred distinctly at slightly lower n_{up} than n_{up} at which $I_{div,LFS}$ rolled over.

3. COMPARISON OF DETACHED L-MODE PLASMAS IN THE CARBON AND ILW CONFIGURATIONS

Corresponding cases of detached L-mode plasmas for both JET-C and JET-ILW were obtained in neutral-beam heated, high upper triangularity ($\delta \sim 0.4$) configurations in horizontal divertor plasma configurations, similar to those described in section 2 (Fig1). As close as possible matching machine parameters were chosen for JET-C and JET-ILW: I_P = [2.0 / 2.0] MA, B_T on axis = [3.1/2.9]T, P_{ohm} + P_{NBI} = [3.9 / 3.5] MW. The resulting power across the separatrix was about 3.4MW for JET-C wall and 3.1MW for JET-ILW (Fig.3a). These plasmas were continuously fuelled with deuterium from the divertor region keeping the magnetic configurations including the strike point positions stationary. In both case $P_{rad,SOL}$ and $P_{rad,div}$ increased nearly linearly with n_{up}, and in JET-ILW saturated just below the density limit (Fig.3a): $P_{rad,div}$ was consistently lower by up 50% in JET-ILW than in JET-C (FIG. 3b). For both materials configurations the density limit occurred at a radiated power fraction of about 50% of the total input power, and at about 20% lower n_{up} for the JET-C, consistent with additional investigations into the density limits [7].

The rollover of $I_{div,HFS}$ and $I_{div,LFS}$ into detachment occurred at 30% higher n_{up} in JET-ILW than in JET-C (Fig.3c and 3d). At matched input power the difference in the rollover density between the two materials configurations are likely to be somewhat smaller; however, it can still be assumed distinctly higher in JET-ILW. Most notably, for both materials configurations the rollover of I_{div} at the HFS and LFS occurred at the same n_{up}. At the rollover density $P_{rad,SOL}$ was of the order 1.2MW for both materials cases, corresponding to a radiated power fraction of 35% and 42% for JET-C and JET-ILW, respectively. This is somewhat lower than what was observed in the low-triangularity configuration in JET-ILW. Beyond rollover, I_{div} at the HFS decreased with increasing n_{up} by an order of magnitude for both materials configurations. At the LFS and for JET-ILW, $I_{div,LFS}$ steadily decreased with n_{up} and was reduced by a factor of 2 compared to its peak value at rollover. In comparison, in JET-C $I_{div,LFS}$ saturated when increasing n_{up} past rollover, and only decreased by 25% close to the density limit. The continuous increase in the degree of detachment with n_{up} in JET-

ILW – constituting itself in 30% higher n_{up} past rollover – permitted operation of partially and fully detached divertor plasmas in a much more stable fashion in JET-ILW than in JET-C. Measurements of P_{div} and $T_{e,LFS}$ of the detail required for making a quantitative assessment do unfortunately not exist for these plasmas.

4. COMPARISON OF DIVERTOR PLASMA CONFIGURATIONS

The effect of the divertor plasma configuration on the divertor conditions was investigated in attached L-mode plasmas in both JET-C wall and JET-ILW, and in ohmically heated, attached and detached plasmas in JET-ILW. Two different divertor plasma configurations were considered: (a) those with the LFS strike point on the horizontal plate, and (b) those with the LFS strike point on the vertical plate (Fig.1). In both configurations, the HFS was on the vertical plate.

For the same upstream conditions, very similar divertor plasma parameters (I_{div}, T_e, and n_e) were measured in the two divertor plasma configurations and for the two materials combinations. For the ohmic plasmas in JET-ILW, the rollover of I_{div} occurred at a SOL radiative power fraction of 40%, consistent with the L-mode cases. A nearly symmetric dependence of I_{div} at the HFS and LFS plates on n_{up} was observed, in particular for the vertical configuration: both $I_{div,HFS}$ and $I_{div,LFS}$ peaked at the same n_{up} (Fig.4a and 4b). Between the horizontal and vertical configurations, I_{div} rolled over at slightly (~10%) lower n_{up} in the vertical configuration. Similarly, $T_{e,LFS}$ dropped to 5 to 8eV at n_{up} distinctly (~30%) lower than those at the rollover of $I_{div,LFS}$ (Fig.4c); at higher n_{up} $T_{e,LFS}$ dropped further toward 1 eV (the lowest detectable $T_{e,LFS}$ with the Langmuir probes). Stable, partially detached divertor conditions were obtained for n_{up} nearly twice the value at rollover. The density limit was observed 30% higher in the vertical configuration. The divertor plasmas greatly differ, however, in the neutral behaviour: the neutral pressure in the subdivertor (Fig.4d) and the integrated Balmer-α emission across the LFS divertor leg (data not shown) are 3-4 higher in the vertical configuration. Conversely, the vertical configuration is significantly better pumped than the horizontal configuration, which in turn required 3-4 higher fuelling rates (H: 5×10^{21} D_2 ® V: 2×10^{22} D_2) to achieve the same n_{up}.

5. EDGE2D/EIRENE PREDICTIONS OF THE MEASURED RADIATION PROFILES AND DIVERTOR CONDITIONS

Utilising the measured profiles of electron density and temperature obtained at the LFS midplane, the 2-D multi-fluid edge code EDGE2D [3] coupled to the neutral Monte Carlo code EIRENE [4],[5] was executed to predict the radiation profiles and divertor parameters as obtained experimentally. Both the low and high triangularity configurations were modelled [8],[9]; here, emphasis is given to the low-triangularity, horizontal configuration. The two material configurations were adapted as they were, including Be in main chamber and W in the divertor for JET-ILW. The code package was substantially upgraded to include impurity sputtering due to other impurities and revised sputtering yields [10]. Migration of Be from the main chamber into the divertor and re-erosion on

the W surfaces were not modelled, i.e., pristine W surfaces in the divertor were assumed. While this may be an appropriate assumption for the LFS plate, Be-rich surface layers are expected along the HFS plate. W transport was modelled with a six-charge state bundling scheme. Carbon as a third impurity species in the Be/W simulations was yet not invoked, which is to some degree justifiable by the low carbon content observed experimentally. Cross-field drifts (**E**×**B** and **B**×∇B) are not included in these simulations; hence, the analysis focuses on the LFS divertor only. The simulations were executed on two sets of grids: (a) one common grid corresponding to the JET-ILW magnetic configuration to assess the predictions for JET-C and JET-ILW on an otherwise identical setup, and (b) two separate grids corresponding to the magnetic configurations of the actual pulses to compare to the experimental data. A diffusive radial transport model with radially varying coefficients was applied to approximate the measured upstream profiles of n_e, T_e, and T_i for the lowest density case, which are then applied for all the other (higher) densities and to both the C and Be/W simulations. The conditions for the total power crossing the grid core boundary were derived from the power balance in the core (2.2 – 2.8MW).

Fully converged solutions were obtained at densities corresponding to the experimental values of n_e at the separatrix at the LFS mid plane ($n_{e,sep,LFS\text{-}mp}$). In addition, in raising the fuelling rate continuously from a low rate (matching the lowest density in the experiments) up to rates corresponding to the simulated density limit produces sets of quasi steady-state solutions. The fuelling and pump locations were adapted as in the experiments: deuterium molecules were injected either at the top (JET-C) or divertor (JET-ILW), and removed in the corners of the divertor. To simulate detached plasmas, a more complete EIRENE model was employed, which includes both elastic and inelastic collisions between deuterons and deuterium molecules, collisional-radiative rates describing reactions between electrons and deuterium molecules, and reactions involving deuterium radicals (D_2^+) [11]. The inclusion of these reactions produced stable solutions down to T_e of 0.2eV at the LFS plate (compared to 0.9 eV with the previous, linearised version of EDGE2D/EIRENE). For attached plasmas both EIRENE models provided identical solutions.

Switching the wall materials from C to Be/W while keeping all other parameters in the simulations the same leads to an approximate 50% reduction of the total radiated power in the SOL, which is driven by replacing C radiation with (mainly) Be radiation ($P_{rad,C} \approx 4\ P_{rad,Be}$, Fig.5b); deuterium radiation is predicted virtually identical (FIG. 5a). Tungsten radiation only plays a role at $T_{e,sep,LFS} > 100$eV. Correspondingly, the simulations for JET-ILW predict, for low-recycling conditions, 20% higher power to the LFS plate (Fig.5c) and higher $T_{e,sep,LFS}$ (Fig.5e) than their JET-C comparison cases. The effect is diminished in high-recycling conditions. Furthermore, the impact of the wall materials on $I_{div,HFS}$ (not shown) and $I_{div,LFS}$ is negligible (Fig.5d).

For both wall materials cases EDGE2D/EIRENE underestimates the total power radiated in the SOL ($P_{rad,tot}$) by about 50 % (Fig.6a and 6f). For JET-C the discrepancy is even more pronounced when considering the radiation in the divertor only ($P_{rad,tot,div}$, Fig.6b). While experimentally $P_{rad,tot,div}$ increased with $n_{e,sep,LFS\text{-}mp}$, and only saturated at the highest density, the simulations indicate a

reduction of divertor radiation when the divertor plasma is detached. (In the simulations the loss in $P_{rad,tot,div}$ is compensated by an increase in radiation in the main SOL.) Despite the lack of radiation to match the measurements, the predictions also underestimate the power conducted to the LFS plate ($P_{div,LFS}$) for low-recycling conditions in both JET-C and JET-ILW, and for high-recycling and detached conditions in the JET-ILW case (Fig.6c and 6h). Increasing the power crossing the grid core boundary – which is supported by the experimental data for high core densities, thus higher ohmic heating – did not lead to a significant increase in $P_{rad,tot}$. Doing so, however, it moved $P_{div,LFS}$ closer to the measurements. Experimental uncertainties, for example, in the bolometer tomographic reconstructions and spatial integration of the profiles, and measuring very low power fluxes with an infrared camera may explain the observed discrepancies between the measurements and simulations. Inclusion of the cross-field drift terms has also shown to produce higher $P_{rad,SOL}$ in the HFS leg and higher $P_{div,LFS}$ [12] for given n_{up}.

Inclusion of a more comprehensive neutral model in EIRENE was key to achieving rollover of $I_{div,LFS}$ and numerically stable, detached divertor plasmas in the simulations (Fig.6d and 6i, also ref. [Guillemaut_PSI12] for the high-δ cases). Without the model extension, $I_{div,LFS}$ would saturate at a certain (high) level, but not decrease significantly. The reduction of $I_{div,LFS}$ is primarily driven by a significant cooling of plasma immediately adjacent to the plate. Quantitatively, the predictions are within a factor of 2 of the measurements. Simultaneously, introducing the extended EIRENE model also increased the momentum losses by a factor of 2. Raising the power across the grid core boundary had the effect of increasing the magnitude of $I_{div,LFS}$ and shifting the predicted rollover toward higher upstream densities.

With increasing upstream density the predicted peak electron temperature at the LFS plate fell from 70 to 100eV to 0.5eV at the rollover of $I_{div,LFS}$ (Fig.6e and 6j). Further increase of $n_{e,sep,LFS\text{-}mp}$ dropped $T_{e,peak,LFS}$ further toward 0.2eV. As for $I_{div,LFS}$, raising the upstream power shifted the required upstream density for dropping below 1eV to higher values, and thereby moved the predictions away from the experimental data.

For the same $n_{e,sep,LFS\text{-}mp}$ and power across the core grid boundary, the simulations predict significantly (up to an order of magnitude) lower electron temperatures at the separatrix on the LFS plate for the vertical divertor plasma configuration compared to the horizontal configuration. The simulations also show a stronger rate of reduction of $T_{e,sep,LFS}$ with $n_{e,sep,LFS\text{-}mp}$ for the vertical configuration, and rollover of $I_{div,LFS}$ at 20% lower $n_{e,sep,LFS\text{-}mp}$. These results are driven by preferential emission of neutrals from the plates toward the separatrix in the vertical configuration and are consistent with those shown in ref. [13] and therein. The predictions are in qualitative agreement with the measurements obtained in ohmic plasmas (Fig.4), but are much pronounced in the simulations than observed experimentally. The simulations were carried out for the JET-ILW materials configuration, but qualitatively do not differ from predictions for JET-C.

5. SUMMARY

For a set of ohmic and L-mode plasmas in high-recycling conditions, replacing the carbon (JET-C) wall with a Be/W (JET-ILW) wall in JET reduced the radiated power in the divertor by 30%, and correspondingly increased the power conducted to the plate and electron temperature by up to a factor of 2. The reduction in radiated power is consistent with the measured, approximately ten times lower carbon content in the plasma in the JET-ILW. In low-recycling conditions the SOL plasmas are nearly identical between the two materials configurations. The rollover of the divertor ion currents as well as the density limit occurred at approximately 30% higher upstream density in the JET-ILW. Stable detached divertor plasmas with a significantly larger operational window in upstream density space were obtained in JET-ILW: beyond partial detachment, $I_{div,LFS}$ steadily decreased with upstream density and was reduced by a factor of 2 compared to its peak value at rollover; in JET-C a 25% reduction of $I_{div,LFS}$ only was obtained. Rather remarkably, the rollover of $I_{div,HFS}$ and $I_{div,LFS}$ occurred at the same upstream densities for both materials configurations. Nearly identical Balmer-α emissions in the LFS divertor plasmas and subdivertor pressures indicate that the neutral behaviour did not significantly differ between the two materials configurations. Electron temperatures of the order 5eV were obtained at upstream densities distinctly lower (~30%) than those at rollover of $I_{div,LFS}$; they are reduced further to 1 eV, and likely below, when the LFS divertor plasma was fully detached.

For otherwise identical setups, simulations with the edge code package EDGE2D/EIRENE predict a 50% reduction of the radiated power in the SOL, qualitatively consistent with the measurements. For both wall materials the simulations show the rollover of the divertor ion current at intermediate densities and steady decrease when increasing the upstream density beyond that: the rollover is less pronounced in JET-C as observed experimentally. Key to obtaining these results is the inclusion of additional reaction rates relating to deuterium molecules and molecular ions. However, the simulations underestimate the radiated power in the SOL, and in particular the radiated power in the divertor, independent of the materials configuration. The predicted power conducted to the LFS plate is, however, within the uncertainties and limitations of the measurements. For a corresponding vertical configuration and the same upstream conditions as in a horizontal configuration, the simulations predict up to an order of magnitude lower electron temperature at the separatrix on the LFS plate, as observed in previous calculations (ref. [13] and therein).

ACKNOWLEDGMENT

This work was supported by EURATOM and carried out within the framework of the European Fusion Development Agreement (EFDA). The views and opinions expressed herein do not necessarily reflect those of the European Commission.

REFERENCES

[1]. Matthews, G.F. et al., Physica Scripta **2011** (2011) 014001.

[2]. Brezinsek, S., et al., Journal of Nuclear Materials **415** (2011) S936.

[3]. Simonini, R., et al., Contribution to Plasma Physics **34** (1994) 368.

[4]. Reiter, D., et al., Journal of Nuclear Materials **196–198 (**1992**)** 80.

[5]. Wiesen, S., JET ITC-Report, http://www.eirene.de/e2deir_report_30jun06.pdf (2006).

[6]. Brezinsek, S., et al., submitted to Journal of Nuclear Materials, August 2012.

[7]. Huber, A., et al., submitted to Journal of Nuclear Materials, August 2012.

[8]. Groth, M., et al., submitted to Journal of Nuclear Materials, August 2012.

[9]. Guillemaut, C., et al., submitted to Journal of Nuclear Materials, August 2012.

[10]. Harting, D., et al., submitted to Journal of Nuclear Materials, August 2012.

[11]. Kotov, V., et al., Plasma Physics and Controlled Fusion **50** (2008) 105012.

[12]. Coster, D.P., et al., *Proc. 32nd EPS Conf. on Plasma Physics* (2012) P1.008.

[13]. Loarte, A., Plasma Physics and Controlled Fusion **43** (2001) R183.

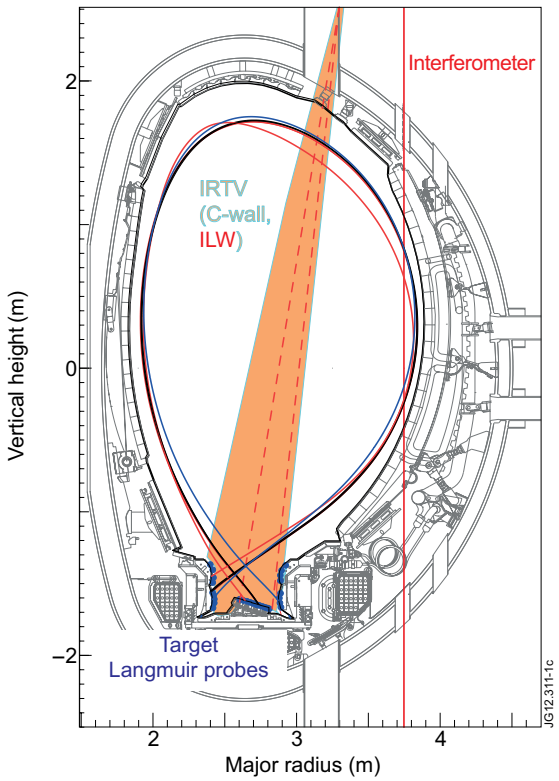

Figure 1: Magnetic equilibria (separatrix) of the low (black, blue) and high triangularity discharges (red), and horizontal (black, red) and vertical (blue) divertor plasma configurations. Some of the principal diagnostics used in these studies are also shown.

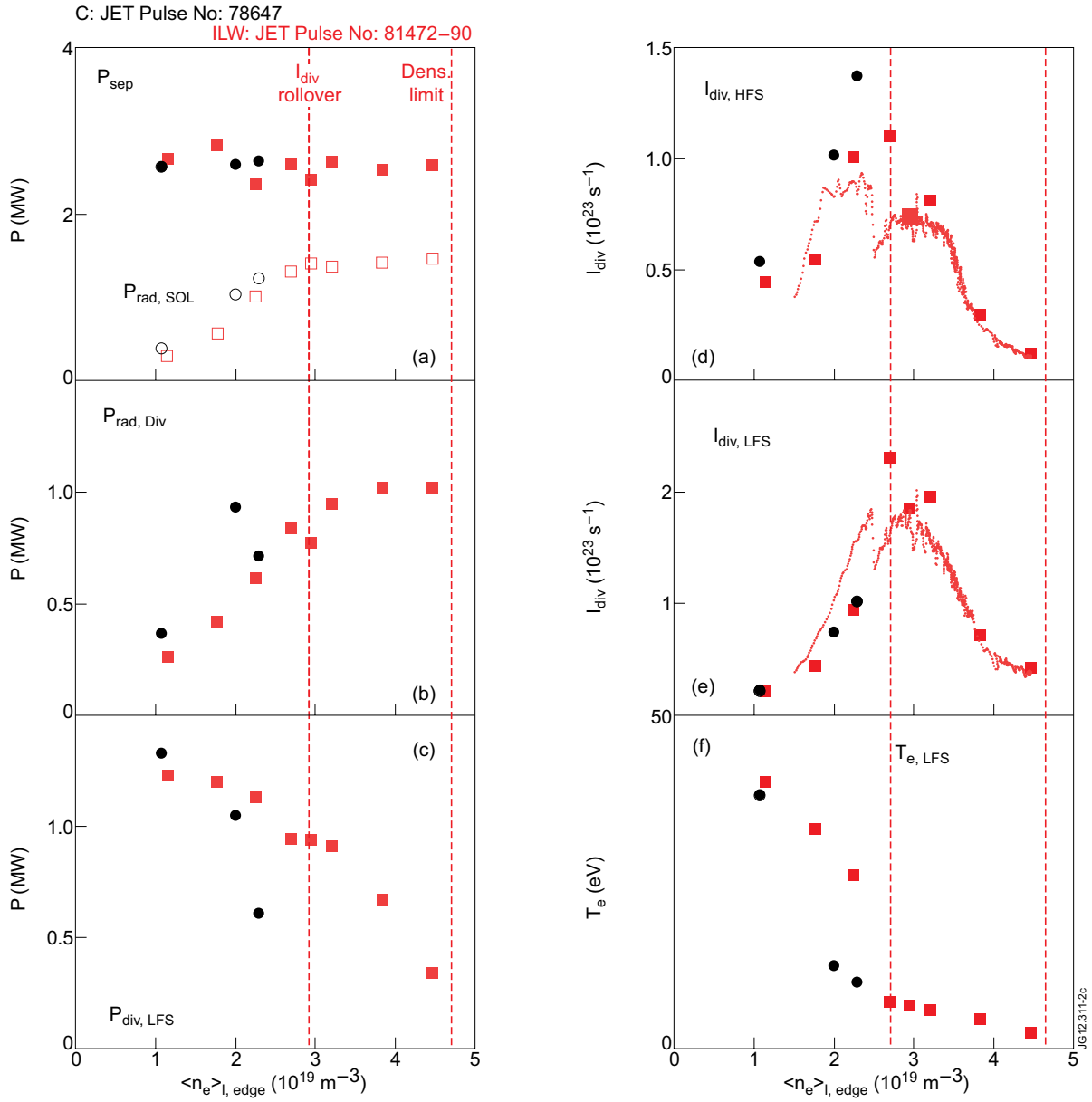

Figure 2: Total power across separatrix and radiated power in the SOL (a), radiated power in the divertor (b), total conducted power to the LFS plate (c), total ion currents to the HFS (d) and LFS (e) plates, and peak electron temperature at the LFS plate (f) as function of line-averaged edge density. Black symbols refer to JET-C, the red symbols to JET-ILW.

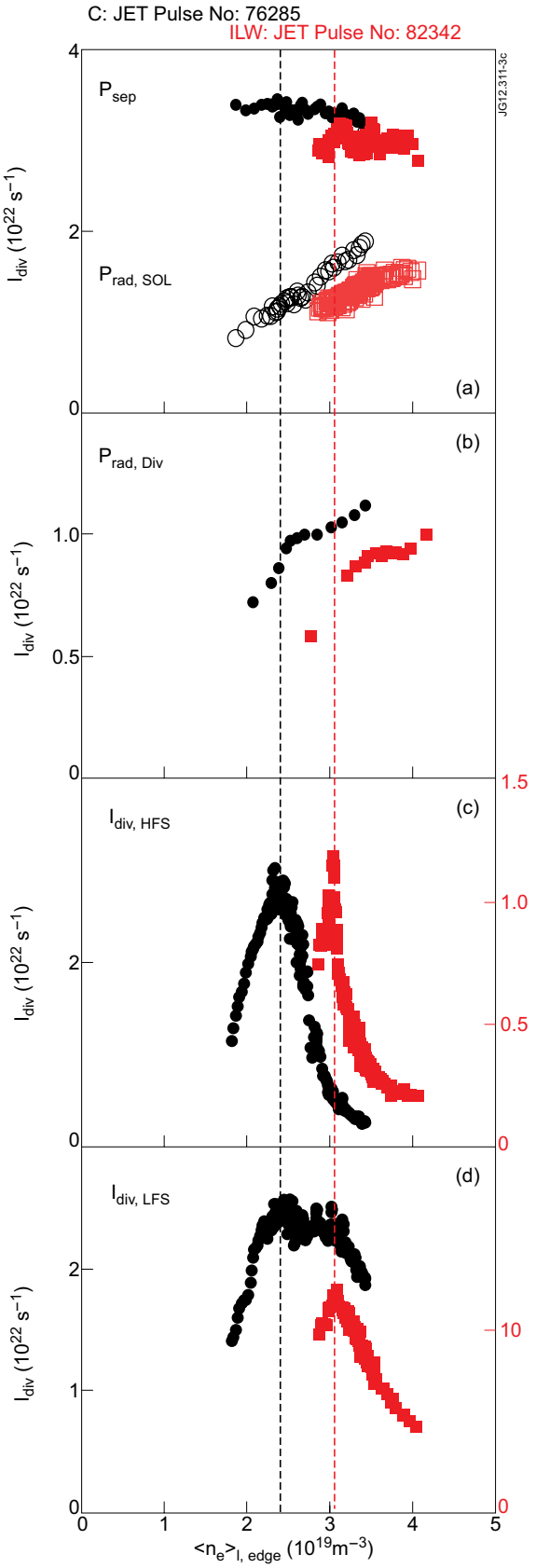

Figure 3: Total power across the separatrix and radiated power in the SOL (a), total radiated power in divertor (b), and total ion currents to the HFS (c) and LFS plates (d) as function of line-averaged edge density. Colours as in Fig.2.

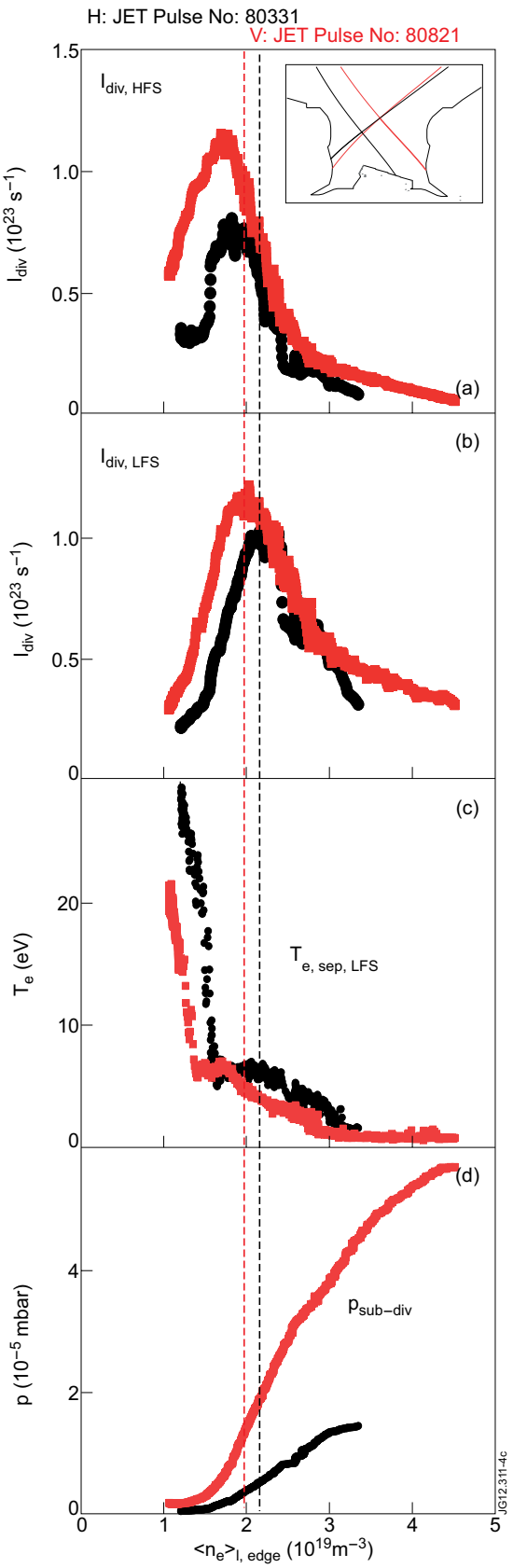

Figure 4: Total ion currents to the HFS (a) and LFS (b) plates, electron temperature at the LFS plate separatrix (c), and total pressure in the subdivertor near the cryo pump (d) as function of line-averaged upstream density. Black symbols refer to the horizontal configuration, red symbols to the vertical one.

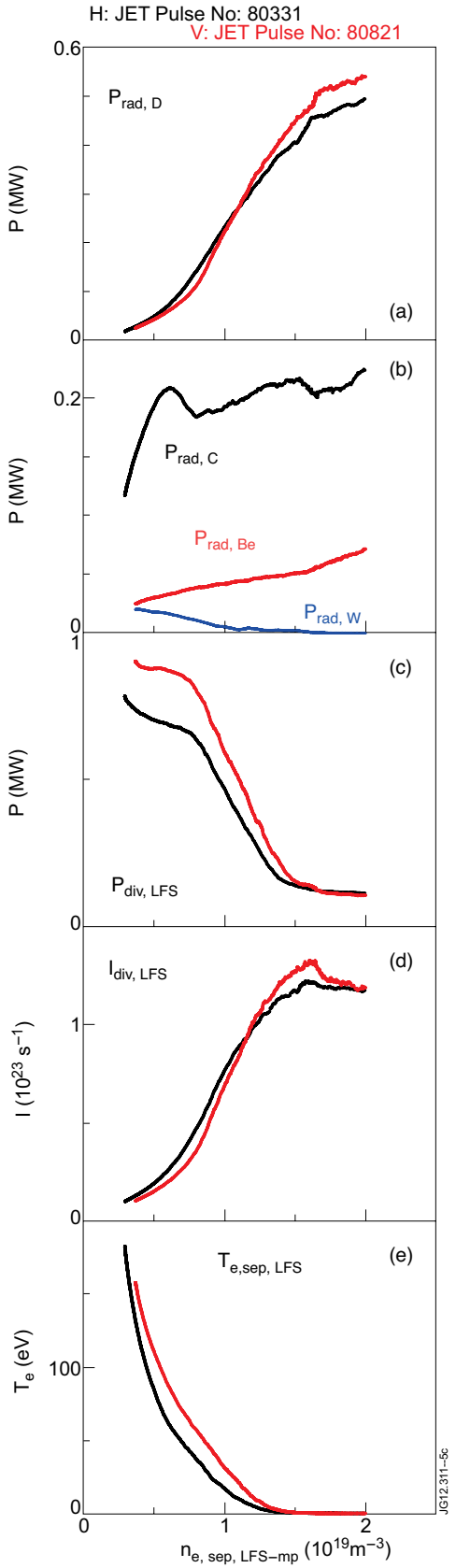

Figure 5: EDGE2D/EIRENE predictions of the total radiated power in D (a) and in C, Be, W (b), conducted power to the LFS plate (c), total ion current to the LFS plate (d), and T_e at the LFS plate separatrix (e) as function of upstream density. The black curves refer to the C case, the red to the ILW one. Low and high recycling conditions only with previous EIRENE model.

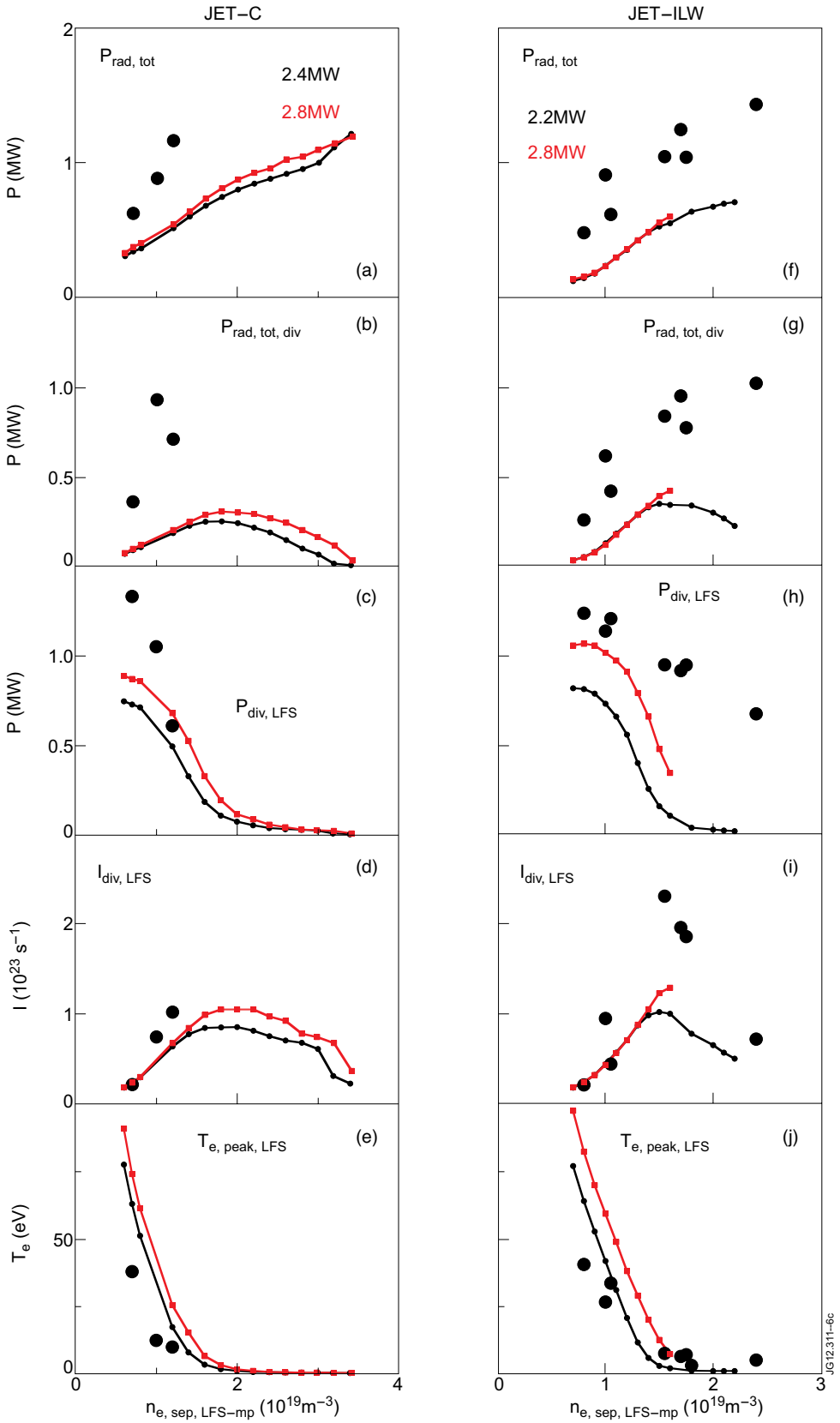

Figure 6: Comparison of the measured (symbols) and predicted (lines) total radiated power in the SOL (a,f), total radiated power in the divertor (b,g), conducted power to the LFS plate (c,h), total ion currents to the LFS plates (d,i), and peak electron temperature (e,j) for the C wall (left column) and ILW (right column) L-mode plasmas in horizontal configuration. The simulated curves in black and right indicate the lower and upper bounds of the assumed power across the grid core boundary.